



Enhanced crystallization rate of bio-based poly(butylene succinate-co-propylene succinate) copolymers motivated by glycerol

Hsu-I. Mao¹ · Li-Yuan Wang¹ · Chin-Wen Chen¹ · Kai-Hung Hsu¹ · Cheng-Hang Tsai¹ · Chia-Jung Cho¹ · Yang-Yen Yu² · Syang-Peng Rwei¹ · Chi-Ching Kuo¹

Received: 21 October 2020 / Accepted: 18 February 2021 / Published online: 21 February 2021
© The Polymer Society, Taipei 2021

Abstract

Isothermal crystallization kinetics are performed in poly(butylene succinate-co-propylene succinate) (PBSPS) in a BS/PS ratio of 10/0(PBS) to 7/3 with 0 and 0.02 mol% glycerol, indicating PBSPS copolymers are 3D growths initiated by heterogeneous nucleation. Crystallization growth rates of BS/PS = 10/0(PBS) to 7/3 with 0.02 mol% glycerol are faster than with 0 mol% glycerol, for a given temperature range. Nonisothermal crystallization kinetics are performed to clarify the effects of different glycerol proportions for BS/PS = 7/3. The 0.01 mol% glycerol is used to form a nucleation site, in which the kinetic energy of the molecular chain can be driven to increase the packing ability. When glycerol is increased to 0.02 mol%, the restriction of the glycerol on the movement of the molecular chain becomes more extensive to decrease the relative crystallinity. Hence, a small amount of glycerol content can improve the relative crystallinity and crystallization rate of PBSPS copolymer.

Keywords Poly(butylene succinate-co-propylene succinate) · Copolymer · Glycerol · Crosslinked

Introduction

The widespread applications of nondegradable plastics have become an increasingly severe problem in the global environment as society and technology develop. Therefore, aliphatic polyester has attracted the attention of numerous researchers as a promising biodegradable material [1–13]. Poly(butylene succinate) (PBS) [14–20] is considered one of the most critical biodegradable materials, and it is widely consumed in industrial applications because of its excellent mechanical properties, thermal stability, and thermal

processability. However, it has a slower biodegradation rate than other aliphatic polyesters because of the high degree of crystallinity. Incorporating second comonomers is an effective approach to modifying the PBS chemical and physical properties.

Biodegradable aliphatic PBS-based copolymers have been developed, such as poly(butylene succinate-co-ethylene succinate) (PBSES) [21, 22], poly(butylene succinate-co-diethylene glycol succinate) (PBSDEGS) [23], poly(butylene succinate-co-hexamethylene succinate) (PBSHS) [21, 24], poly(butylene succinate-co-decamethylene succinate) (PBSDS) [25], poly(butylene succinate-co-2-methyl-1,3-propylene succinate) (PBSMPS) [26, 27], poly(butylene succinate-co-neopentyl glycol succinate) (PBSNPGS) [28]. Poly(propylene succinate) (PPS) [29–31] consists of 1,3-propanediol and succinic acid displays a relatively high biodegradation rate. However, it also displays a low melting point and low crystallinity compared with two or four methylene groups in the diol monomer because of the odd number of methylene groups. Poly(butylene succinate-co-propylene succinate) (PBSPS) has been synthesized and characterized to combine the individual advantages of PBS and PPS. Papageorgiou and Bikiaris copolymerized a series of

Hsu-I. Mao and Li-Yuan Wang are equally contributed to this work.

✉ Chin-Wen Chen
cwchen@ntut.edu.tw

✉ Chi-Ching Kuo
kuocc@mail.ntut.edu.tw

¹ Institute of Organic and Polymeric Materials, Research and Development Center of Smart Textile Technology, National Taipei University of Technology, No. 1, Sec. 3, Chung-Hsiao East Road, Taipei 10608, Taiwan

² Department of Materials Engineering, Ming Chi University of Technology, New Taipei City 24301, Taiwan

PBSPS with a variety of BS/PS concentration to observe the eutectic and multiple melting behaviors. A banded spherulite was obtained, and the space between bands increased with crystallization temperature [32]. PBSPS was produced by Xu's group, suggesting that PS units lowered the regularity of the molecular chain to reduce the thermal property [33]. Furthermore, the isothermal crystallization behavior of PBSPS was analyzed using the Avrami model, which revealed Avrami exponents in the range of 2.2–2.8, reflecting heterogeneous nucleation and three-dimension growth of the crystal structure [34]. Lu et al. proposed PBSPS with BS/PS = 95/5 and 90/10. BS/PS in a ratio of 90/10 had a growth rate that was 1/7 that of PBS, and BS/PS = 95/5 had a growth rate of 1/3 that of PBS at 80 °C [35]. A small amount of crosslinking modification was also performed to improve the properties of copolymers in several systems [36–39].

PBSPS was copolymerized with glycerol (GC) as a partial crosslinking agent to improve the thermal and mechanical properties. Notably, the suitable thermal properties were obtained for GC of 0.01 mol% and then decreased by raising the GC concentration to 0.02–0.03 mol%, indicating a relatively high crystallinity in the concentration [40]. Liu et al. manufactured PBS copolymers with a small amount of crosslinking agent of 5-(2-(trimethylsilyl)ethynyl) isophthalate (DTS) and a concentration of < 1.0%. A higher crystallization rate and T_c of PBDSx than neat PBS was observed, suggesting that the small amount of crosslinking significantly accelerated PBS crystallization. Notably, as the DTS concentration increased, the crystallinity increased initially and then decreased [41]. A crosslinkable comonomer, dimethyl 4,40-(buta-1,3-diyne-1,4-diyl) dibenzoate (DA), was copolymerized with PBS by Liu's group. The DA would act the role as the nucleating agent to drive the crystallization rate [42]. Ma et al. proposed a partial crosslinking PBS with a dicumyl peroxide (DCP) concentration of < 0.5 wt% as initiator. The T_c increased by 15–20 °C when incorporated with DCP of 0.05–0.5 wt%, indicating a high nucleation efficiency. When the DCP concentration exceeded 1.0 wt%, the T_c of polymers was dropped and displayed a broad peak, which can be attributed to the higher gel fraction and crosslinking density that restrict the crystallization process [43].

In this study, the isothermal crystallization of PBSPS copolymers with different ratios of PS to BS segments was examined using differential scanning calorimetry with or without GC of 0.02 mol%. The effect of GC concentration at a fixed BS/PS ratio of 7/3 in various cooling rates was investigated by nonisothermal crystallization. The crystallization kinetics of copolymers was analyzed using Avrami [44, 45] and Mo [46, 47] models. Moreover, the observation of spherulite morphology and crystal growth rate was achieved by polarized light microscopy (PLM).

Materials and methods

Materials

1,4-butanediol (1,4-BDO) (99%) and Glycerol (GC) (99%) were obtained from First Chemical Corporation (Taipei City, Taiwan). 1,3-propanediol (1,3-PDO) (99%) was supplied from MERU Chemical Co. Ltd. (Taipei City, Taiwan). Succinic acid (SA) (99%) was provided by Huachen Chemical Co. Ltd. (Taichung City, Taiwan). Titanium(IV) butoxide ($Ti(OBu)_4$) (97%) was produced by Aldrich (St. Louis, MO, USA).

Synthesis of PBSPS copolymers

PBSPS copolymers were copolymerized via bulk polymerization in two steps using an acid/diol mole ratio of 1/1.1 in a 2 L steel reactor. The succinic acid was synthesized in one pot with 1,4-butanediol, 1,3-propanediol, glycerol, and the catalyst, $Ti(OBu)_4$ in 500 ppm at 180–190 °C for 4 h under constant nitrogen flux for esterification. Later, pre-polycondensation reaction for 0.5 h under 200 torr was performed while the H_2O was collected via a condenser above 90%. After that, the temperature was raised to 230 °C, and the pressure was gradually decreased to 4 torr for the polycondensation procedure. While the torque value grew to 1.25 times by the initial value, indicating that the polycondensation reaction can be terminated and put the melted samples into the iced water bath for cutting to chip shape and further analysis. The synthesis route of PBSPS copolymers displayed in Scheme 1, and all the information in synthesis, characteristic, thermal, and mechanical properties have been published in *Soft Matter*, **2019**, 15, 9710–9720 [40].

Differential scanning calorimetry (DSC)

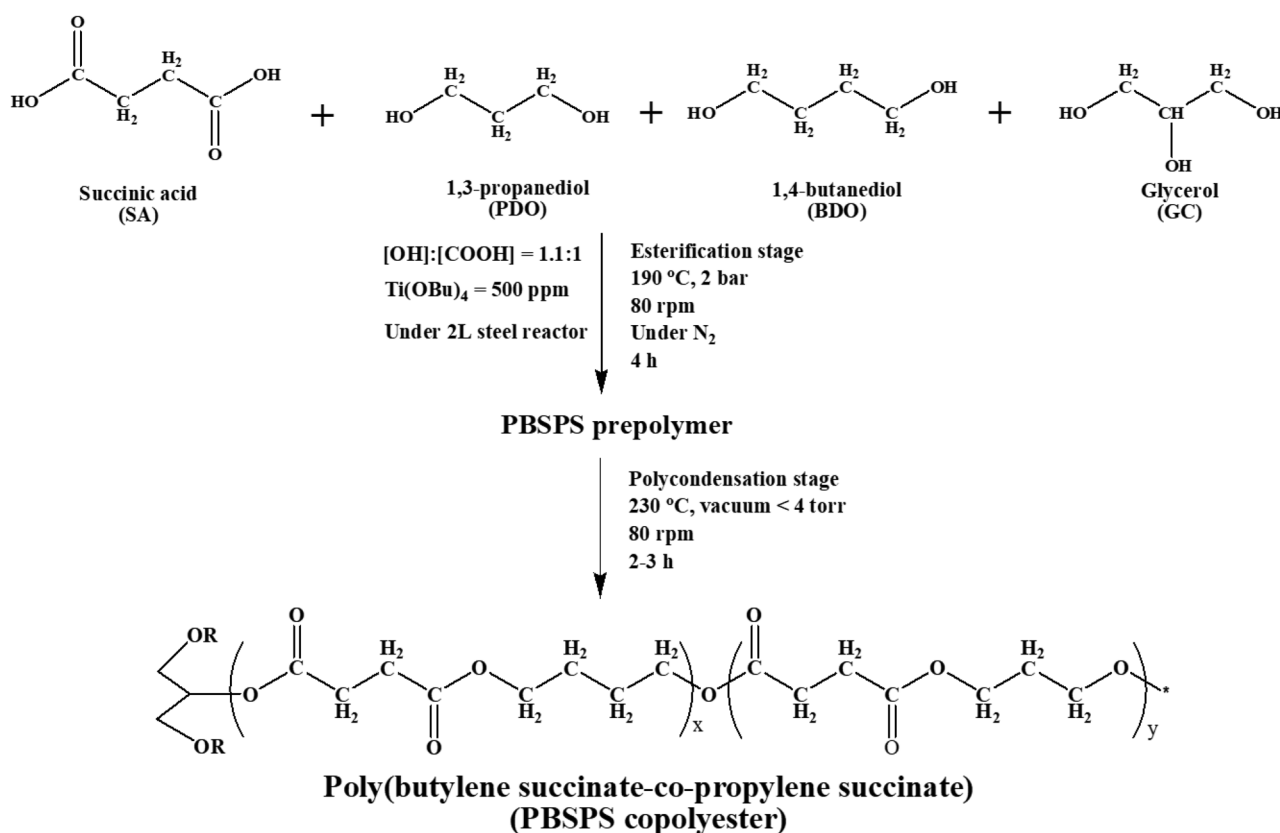
A thermal experiment was carried out via DSC (Hitachi High Tech. DSC-7000, Japan) under N_2 atmosphere.

The DSC measurement of PBSPS copolymers was analyzed in the following sections:

1. Typical thermal properties analysis

PBSPS copolymers were melted at 150 °C for 5 min to eliminate thermal histories, then cooled to –50 °C and reheated to 150 °C under a rate of 10 °C min^{-1} . The crystallization temperature (T_c) and crystallization enthalpy (ΔH_c) were obtained from the cooling round; The melting temperature (T_m) and melting enthalpy (ΔH_m) were analyzed from the reheating round.

2. Isothermal crystallization analysis



Scheme 1 Synthetic routes of poly(butylene succinate-*co*-propylene succinate) copolymers

The PBSPS copolymer was first heated to 150 °C under 10 °C min⁻¹ and held for 5 min to remove the thermal history. Then, the sample was cooled to a given crystallization temperature under a rate of 150 °C min⁻¹ and then kept for 30 min. Later, increased the temperature to 150 °C under a rate of 10 °C min⁻¹, recorded the crystallization status by isothermal, and measured the melting temperature at different given crystallization temperatures [48].

3. Nonisothermal crystallization analysis

PBSPS copolymer was first heated up from -50 to 150 °C under 10 °C min⁻¹ and was held at this temperature for 5 min to eliminate the thermal history and then cooled down to -50 °C under different cooling rate (2.5, 5, 7.5, and 10 °C min⁻¹). The curves of heat flow under cooling and heating process were record.³⁸

Fig. 1 DSC curve of PBSPS copolymers with 0 and 0.02 mol% GC in (a) 1st cooling process and (b) 2nd reheating process at a rate of 10 °C min⁻¹. The feed molar ratio of 1,4-BDO to 1,3-PDO was 10:0, and the ratio of GC was 0 mol%, it was denoted as BS/PS = 10/0(PBS) - 0

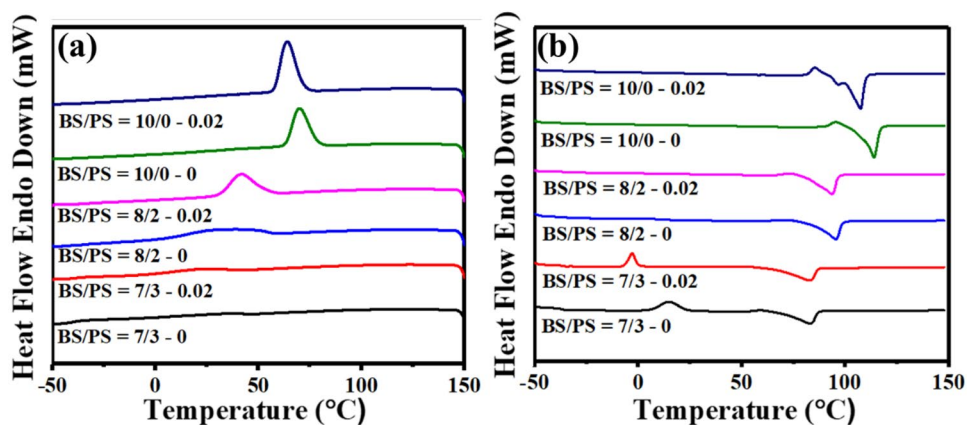


Table 1 Thermal property of PBSPS copolymers with 0 and 0.02 mol% GC at BS/PS concentrations of 10/0(PBS), 8/2, and 7/3

| Sample | T_c (°C) | T_m (°C) | ΔH_{hc} (J g ⁻¹) | ΔH_{cc} (J g ⁻¹) | ΔH_m (J g ⁻¹) |
|------------------------|---------------|---------------|---|---|--------------------------------------|
| BS/PS = 10/0(PBS)-0 | 70.2 | 113.9 | 59.0 | n.a | 68.0 |
| BS/PS = 10/0(PBS)-0.02 | 64.3 | 107.4 | 63.5 | n.a | 73.8 |
| BS/PS = 8/2-0 | 28.0 | 95.7 | 40.9 | n.a | 51.5 |
| BS/PS = 8/2-0.02 | 42.2 | 93.4 | 44.7 | n.a | 49.4 |
| BS/PS = 7/3-0 | 17.8 | 83.0 | 5.4 | 28.1 | 39.2 |
| BS/PS = 7/3-0.02 | 23.6 | 82.9 | 13.0 | 16.7 | 43.2 |

Polarized light microscope (PLM)

The spherulitic morphology of PBSPS copolymers was observed by a polarized light microscope (Nikon ECLIPSE LV100N POL) with a heating stage and liquid nitrogen cooling system. The sample was first heated to 120 °C under 150 °C min⁻¹ and kept for 5 min to erase thermal history, then cooled to specific temperature under 150 °C min⁻¹, and maintained for 30 min. The process of crystallization was recorded by Nikon camera with the NIS Elements imaging software.

Results and discussion

Figure 1 illustrates the DSC traces in different ratios of PBSPS copolymers, with 0 and 0.02 mol% GC, in a temperature range of -50 to 150 °C. BS/PS = 10/0(PBS), 8/2, and 7/3 copolymers displayed both T_m and T_c peaks, as summarized in Table 1. As presented for the first cooling process, the T_c decreases as the PS ratio increases in PBSPS copolymer. The overall ΔH_m is reduced, indicating a decrease in the crystallinity and the crystallization behaviors associated with the PS unit. As expected, the T_m decreases

Table 2 Thermal property of PBSPS copolymers with different ratios of GC at BS/PS concentrations of 7/3

| Sample | T_c (°C) | T_m (°C) | ΔH_{hc} (J g ⁻¹) | ΔH_{cc} (J g ⁻¹) | ΔH_m (J g ⁻¹) |
|------------------|---------------|---------------|---|---|--------------------------------------|
| BS/PS = 7/3-0 | 17.8 | 83.0 | 5.4 | 28.1 | 39.2 |
| BS/PS = 7/3-0.01 | 26.0 | 83.9 | 36.2 | 3.2 | 42.6 |
| BS/PS = 7/3-0.02 | 23.6 | 82.9 | 13.0 | 16.7 | 43.2 |
| BS/PS = 7/3-0.03 | 23.8 | 79.5 | 2.7 | 28.7 | 38.4 |

with the increase in the PS concentration in PBSPS copolymer in the second reheating procedure. T_{cc} occurs at BS/PS = 7/3 during the heating process.

Figure 2 displays the DSC traces of PBSPS copolymers with different concentrations of GC in a temperature range of -50 to 150 °C; all the thermal properties are recorded in Table 2. The composition of GC increases from 0 to 0.01 mol%, indicating that fewer nodes are located in the networking structure to drive the molecular chains to be softer and well packaged, resulting in larger T_c and ΔH_m . The GC ratio is improved by > 0.01 mol%; however, the increase of nodes restricts the chain movement and makes stacking difficult, causing a smaller T_{hc} and ΔH_m . Finally, a small amount of GC inside PBSPS copolymers appears to affect the crystallinity and drive the crystallization rate.

Figure 3 illustrates the DSC trace of PBSPS copolymers with different ratios of BS/PS and different concentrations of GC at various temperatures. All the PBSPS copolymer's crystallization peaks shift to the right and flatten as the crystallization temperature increases, suggesting that PBSPS copolymer requires more time to complete crystallization under higher crystallization temperatures. The heat flow curve of the copolymer with 0 mol% GC is flatter than the copolymer with 0.02 mol% GC. Therefore, the crystal growth space within the copolymer is obstructed by the presence of the GC as a crosslinking agent. Therefore, a copolymer with a GC = 0.02 mol% requires a large amount

Fig. 2 DSC curve of BS/PS = 7/3 copolymers with different ratios of GC in (a) 1st cooling process and (b) 2nd reheating process at a rate of 10 °C min⁻¹

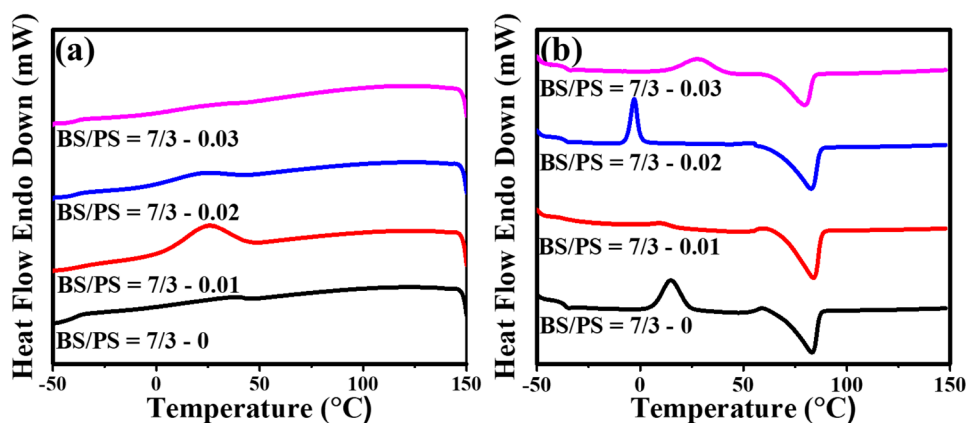
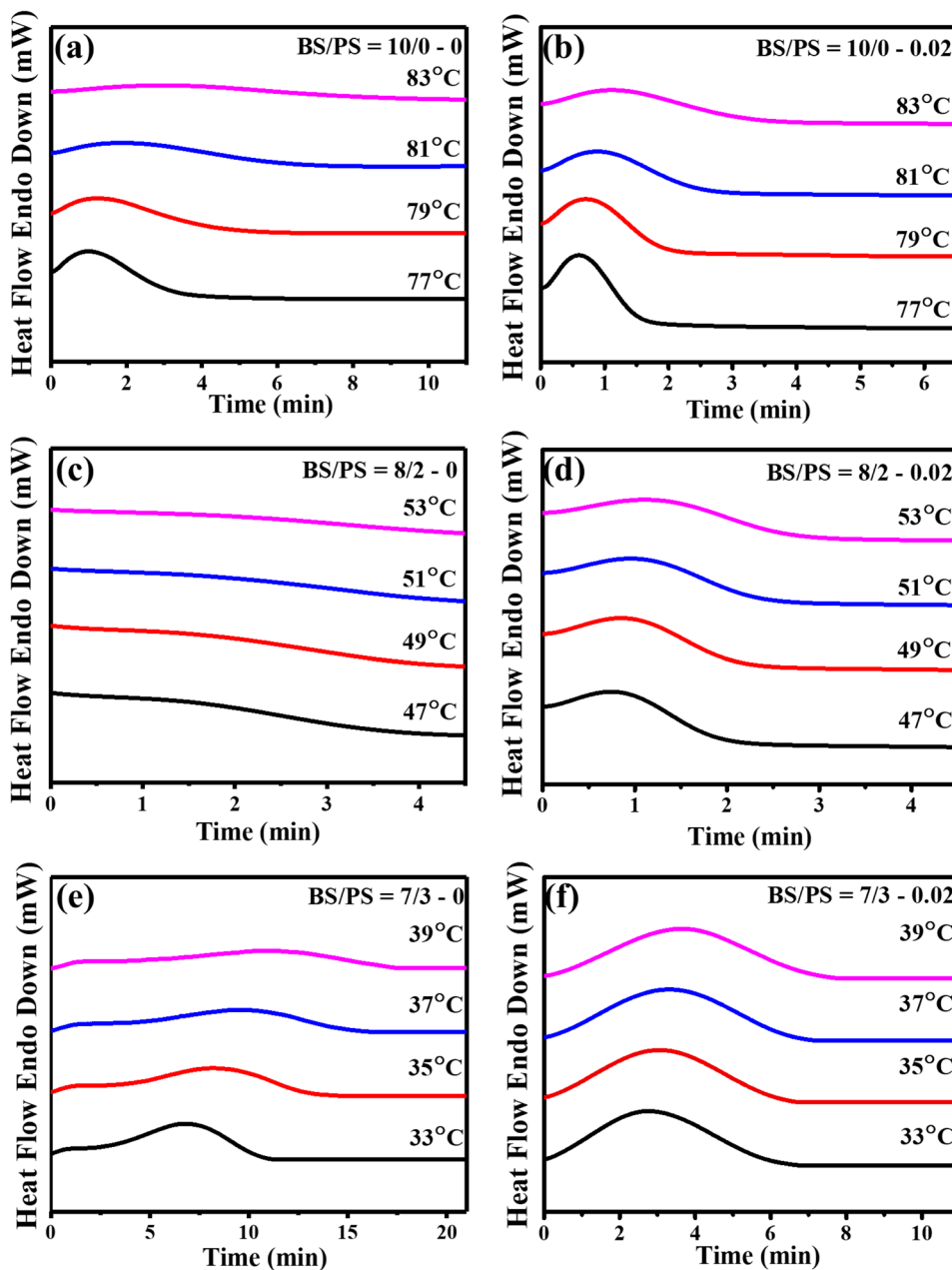


Fig. 3 DSC curve of PBSPS copolymers with different ratios of BS/PS and different concentrations of GC in the isothermal crystallization at given temperatures. (a) BS/PS = 10/0(PBS) – 0, (b) BS/PS = 10/0(PBS) – 0.02, (c) BS/PS = 8/2 – 0, (d) BS/PS = 8/2 – 0.02, (e) BS/PS = 7/3 – 0, and (f) BS/PS = 7/3 – 0.02



of energy during the isothermal crystallization process, and the time required for crystallization is short.

The evolution of crystallinity is related to the change of enthalpy during crystallization. The relative crystallinity, $X(t)$, at different crystallization times could be obtained from the exothermic to time area and the total exotherm with an equation as follows:

$$X(t) = \frac{X_C(t)}{X_C(t_\infty)} = \frac{\int_0^t \frac{dH(t)}{dt} dt}{\int_0^\infty \frac{dH(t)}{dt} dt} \tag{1}$$

where $dH(t)/dt$ denotes the rate of heat flow, reveals that $dH(t)$ is the enthalpy of crystallization at a certain temperature during the time interval dt via DSC measurement.

The exothermic heat during the polymer chain stack into an ordered state to form a crystallization regime was measured, which could be analyzed by DSC and determined using the Avrami model, the equation described as follows:

$$X(t) = 1 - \exp(-kt^n) \tag{2}$$

$$\log\{-\ln[1 - x(t)]\} = -\log k + n \log t \tag{3}$$

where $X(t)$ is the relative crystallinity at different crystallization time t , k is the nucleation and growth rate parameters, and n can display that the nucleation and growth geometry of the crystals.

The isothermal crystallization behaviors of PBSPS copolymers with GC are investigated using temperature ranges of 77–83, 47–53, and 33–39 °C for BS/PS = 10/0(PBS), 8/2, and 7/3, respectively, as presented in Fig. S1. The crystallization rate of PBSPS copolymers decreases as the proportion of PS increases. Furthermore, the relative crystallinity over time for PBSPS copolymer in different ratios of GC, as well as all the characteristic isothermal curves are shifted to the right along the time axis as the isothermal temperature increases.

All the experimental data were transformed with $\log(-\ln(1 - X(t)))$ as a function of $\log(t)$, at $X(t)$ in the range of 20%–80%, and were fitted at various temperatures by the Avrami equation, as introduced in Fig. S2. The Avrami equation parameters, n and k , were linearly regressed to obtain the slopes and intercepts of the curve for PBSPS copolymers at various temperatures. The half-time and growth rates were determined using Eq. (4) or (5), and the detailed data are summarized in Table 3. The n values of the Avrami exponent were approximately 2.01–3.50 in all the

PBSPS copolymers, in which a heterogeneous nucleation mechanism causes three-dimensional growth, and the crystal morphology is spherulite. Furthermore, the n and k values have distinct trends in PBSPS copolymers with 0 and 0.02 mol% GC, revealing that a possible significant role of GC in the crystallization rate and morphology inside the BS and PS molecules. The $t_{1/2}$ and G values demonstrate a faster crystallization rate in the presence of GC in 0.02 mol% than in the neat PBSPS copolymer at a given temperature, indicating that the crystallization rate could be improved by inserting GC into PBSPS copolymers. Compare to the ΔE values of samples with 0 and 0.02 mol% GC, higher ΔE values were observed after the addition of GC, demonstrating a similar tendency with Avrami analysis.

$$t_{1/2} = (\ln 2/k)^{1/n} \quad (4)$$

$$G = 1/t_{1/2} \quad (5)$$

Figure 4 illustrates the growth rate of crystallization at different temperatures. The trend of the crystal growth rate for PBSPS copolymer with 0 mol% GC is < 0.02 mol% GC, under the same BS/PS ratio. However, the presence of GC has a significant effect on the crystal growth rate

Table 3 Avrami analysis for isothermal crystallization and half-time of crystallization for PBSPS copolymers with GC at different BS/PS concentrations

| Sample | Temp (°C) | n | k (min ⁻ⁿ) | $t_{1/2}$ (min) | G (min ⁻¹) | ΔE (kJ mole ⁻¹) |
|------------------------|-----------|------|--------------------------|-----------------|--------------------------|-------------------------------------|
| BS/PS = 10/0(PBS)-0 | 77 | 2.12 | 0.3889 | 1.3137 | 0.7612 | -182.5 |
| | 79 | 2.01 | 0.2388 | 1.6987 | 0.5887 | |
| | 81 | 2.06 | 0.0999 | 2.5555 | 0.3913 | |
| | 83 | 2.22 | 0.0369 | 3.7441 | 0.2671 | |
| BS/PS = 10/0(PBS)-0.02 | 77 | 2.43 | 1.6192 | 0.7058 | 1.4169 | -121.1 |
| | 79 | 2.31 | 1.0087 | 0.8501 | 1.1763 | |
| | 81 | 2.28 | 0.5776 | 1.0831 | 0.9232 | |
| | 83 | 2.27 | 0.3223 | 1.4021 | 0.7132 | |
| BS/PS = 8/2-0 | 47 | 2.68 | 0.1866 | 1.6308 | 0.6132 | -81.2 |
| | 49 | 2.70 | 0.1428 | 1.7967 | 0.5566 | |
| | 51 | 2.55 | 0.1319 | 1.9176 | 0.5215 | |
| | 53 | 2.58 | 0.1115 | 2.0281 | 0.4931 | |
| BS/PS = 8/2-0.02 | 47 | 2.50 | 0.9114 | 0.8961 | 1.2102 | -52.1 |
| | 49 | 2.52 | 0.6957 | 0.9986 | 1.1159 | |
| | 51 | 2.53 | 0.5205 | 1.1197 | 1.0014 | |
| | 53 | 2.54 | 0.3626 | 1.2904 | 0.8931 | |
| BS/PS = 7/3-0 | 33 | 3.50 | 0.0011 | 6.3805 | 0.1567 | -56.5 |
| | 35 | 3.23 | 0.0010 | 7.6626 | 0.1305 | |
| | 37 | 3.10 | 0.0009 | 8.6623 | 0.1154 | |
| | 39 | 3.00 | 0.0008 | 9.6519 | 0.1036 | |
| BS/PS = 7/3-0.02 | 33 | 2.50 | 0.0457 | 2.9649 | 0.3373 | -27.1 |
| | 35 | 2.58 | 0.0362 | 3.1363 | 0.3189 | |
| | 37 | 2.61 | 0.0290 | 3.3737 | 0.2964 | |
| | 39 | 2.67 | 0.0217 | 3.6670 | 0.2727 | |

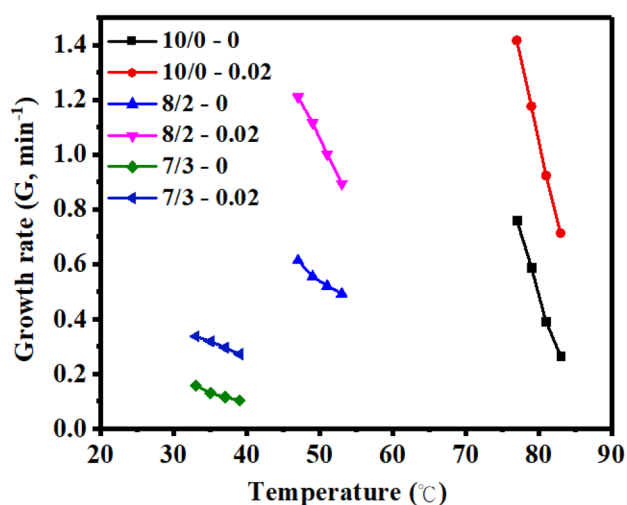


Fig. 4 Growth rate of crystallization (G in the unit of min^{-1}) as a function of temperature for PBSPS copolymers with GC at different concentrations of BS/PS

of the copolymers. This observation may indicate that a higher crystallization growth rate is obtained when a small amount of GC ratio exists as a nucleation point to reduce the chain movement, which is beneficial to the stacking of the molecular chain and facilitates crystallization [41–43].

The PLM image of PBSPS copolymers is displayed in Figs. 5 and 6 for BS/PS = 10/0(PBS) and 7/3, respectively. PBSPS copolymers are cooled to the crystallization temperature and maintained at the temperature by isothermal crystallization, and a spherulite crystal can be identified using PLM observation. Furthermore, when BS/

PS = 10/0(PBS), the spherulite forms more completely because the PS unit is not involved. If the PS ratio is increased to BS/PS = 7/3, the addition of the PS unit may disturb the crystal structure during the growth process, which causes the formation of a smaller spherulite.

The isothermal crystallization method was employed to investigate the influence of GC concentrations, which reveals that the crystallization rate of all samples increases with the incorporation of 0.02 mol% GC. Therefore, the GC concentrations in 0, 0.01, 0.02, and 0.03 mol% into BS/PS = 7/3 on the crystallization behavior of PBSPS copolymers were examined by nonisothermal crystallization kinetics. PBSPS copolymers cooling at 2.5, 5, 7.5, or 10 $^{\circ}\text{C min}^{-1}$, and then heating at 10 $^{\circ}\text{C min}^{-1}$ was performed with DSC machines. BS/PS = 10/0(PBS), and 8/2 without and with 0.02 mol% GC were observed in a single peak during the cooling process, as illustrated in Figs. 7 and S3. The exothermic peak shifts to a lower temperature and becomes wider as the cooling rate increases, indicating that the motion of the molecular chain is not rapid enough to reach thermal equilibrium at the fast cooling rate. The enthalpy of peaks is itemized in Table S1, revealing BS/PS = 10/0(PBS), with GC = 0.02 mol% display 64.3, 64.1, 64.0, and 63.5 J g^{-1} under cooling rates of 2.5, 5, 7.5, 10 $^{\circ}\text{C min}^{-1}$, respectively, indicating that similar degrees of crystallization are achieved.

Figure 8 displays DSC curves of the BS/PS = 7/3 copolymers with GC concentrations of 0, 0.01, 0.02, and 0.03 mol%. The cooling crystallization peaks of samples become weaker as the cooling rate increases; therefore, a more substantial crystallization peak is observed in the second reheating process, and comparable values

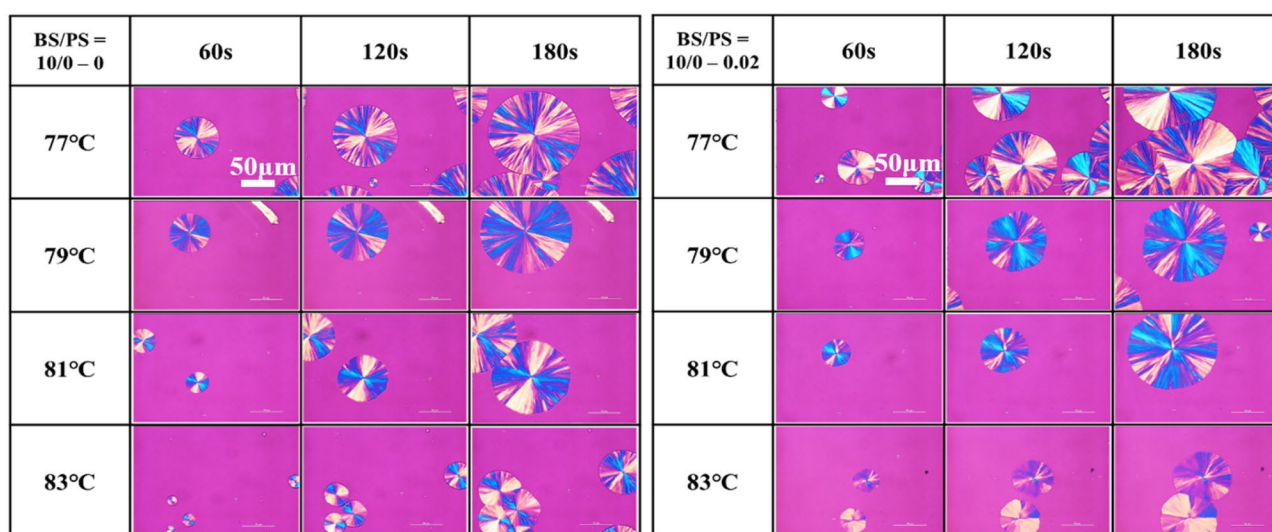


Fig. 5 PLM image of BS/PS = 10/0(PBS)—0 and 0.02 polymers in the isothermal crystallization by time evolution at a given temperature as a function of time

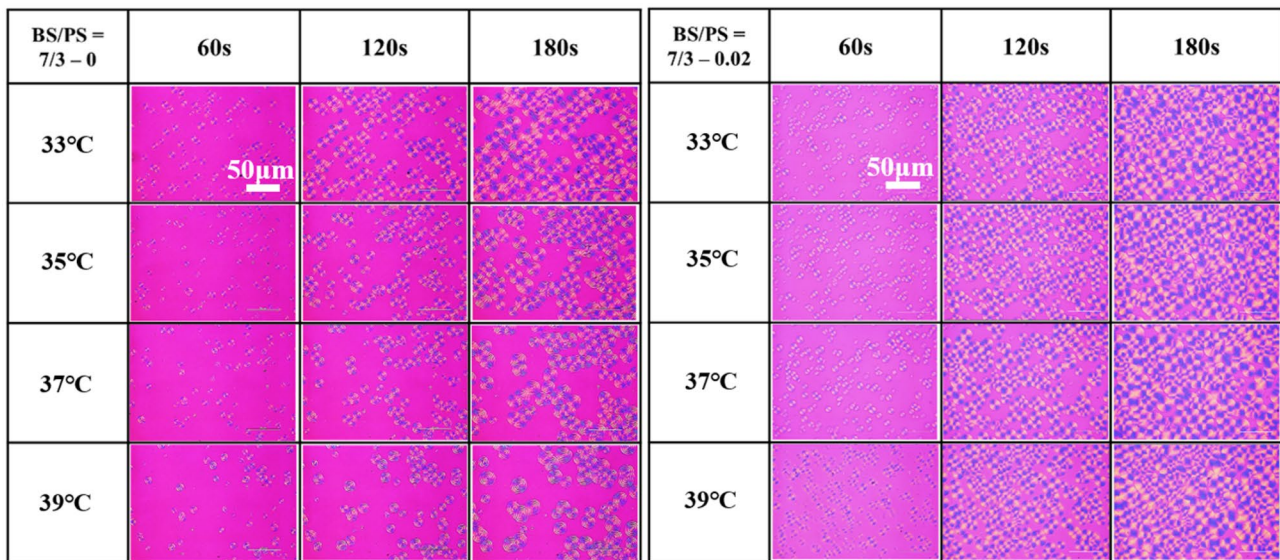


Fig. 6 PLM image of BS/PS = 7/3—0 and 0.02 copolymers in the isothermal crystallization by time evolution at a given temperature as a function of time

of ΔH_m are obtained. (e.g., when BS/PS = 7/3 with GC = 0.02 mol%, ΔH_{hc} is 37.7, 36.6, 23.2, and 13 J g⁻¹; ΔH_{cc} is 0, 0.29, 7.59, and 16.7 J g⁻¹; and ΔH_m is 40.8, 41.9, 42.1, and 41.1 J g⁻¹ at 2.5, 5, 7.5, and 10 °C min⁻¹,

respectively.) All the data are tabulated in Table S2. The results indicate that the chain is not easily packed into a crystal region under a faster cooling rate, which would result in a lower ΔH_{hc} value, and thus demonstrate lower

Fig. 7 DSC curve of PBSPS copolymers in the cooling process at 2.5, 5, 7.5, 10 °C min⁻¹ (a) BS/PS = 10/0(PBS) - 0, (b) BS/PS = 10/0(PBS) - 0.02, (c) BS/PS = 8/2 - 0, (d) BS/PS = 8/2 - 0.02

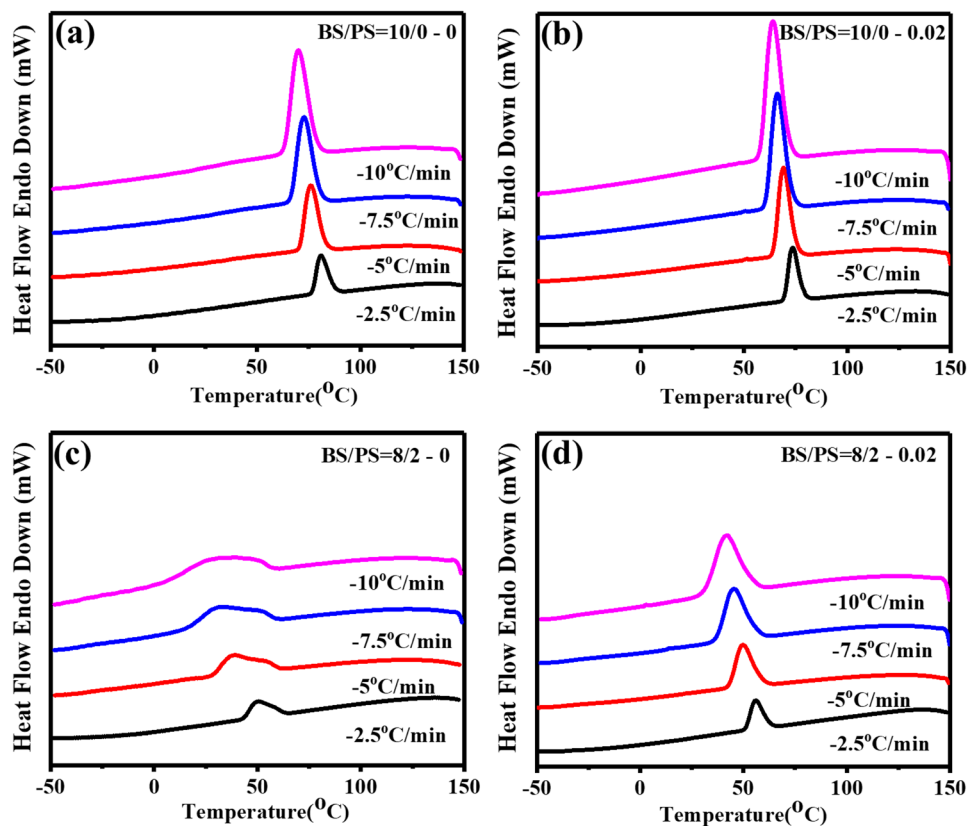
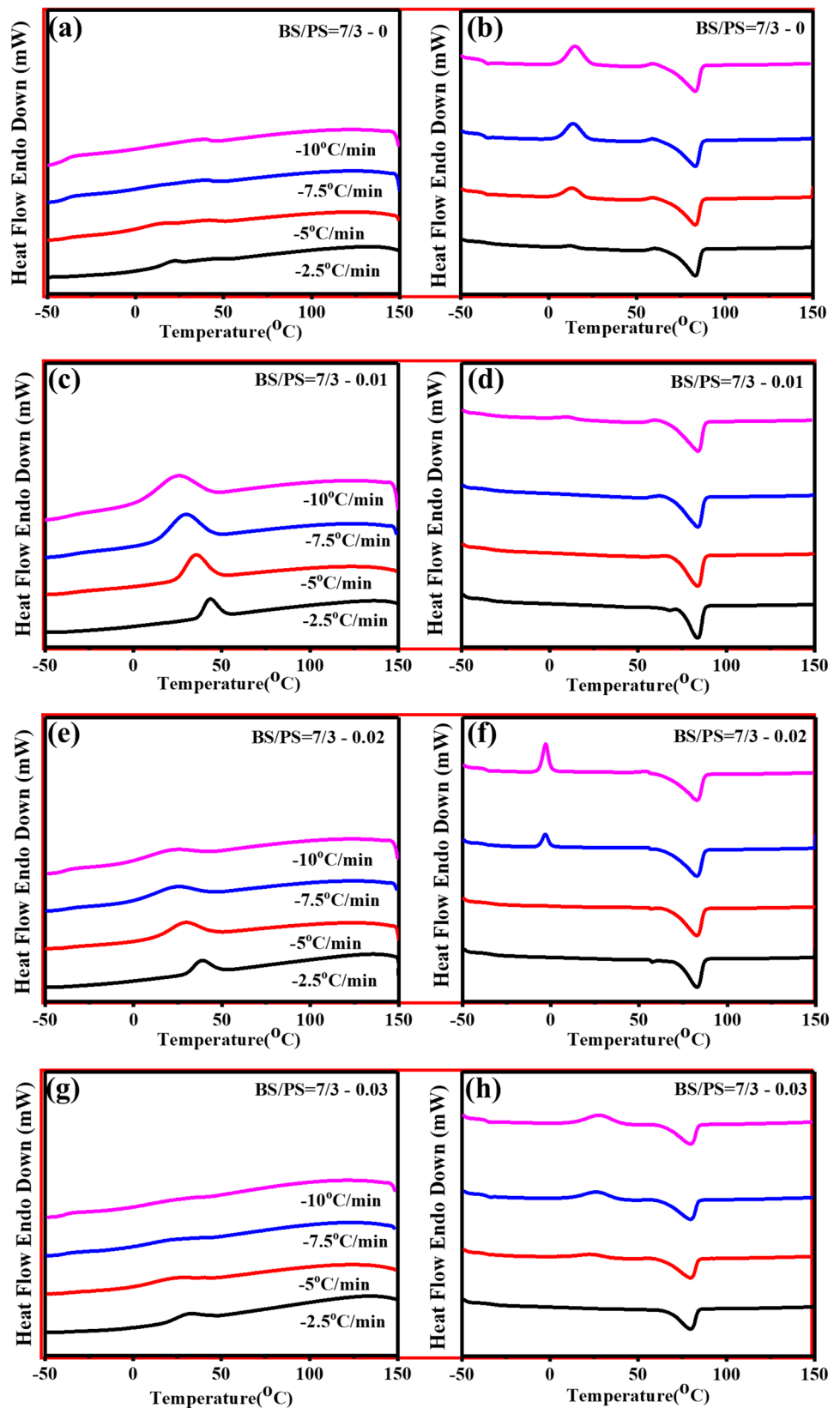


Fig. 8 DSC curve of PBSPS copolymers in cooling process at 2.5, 5, 7.5, 10 °C min⁻¹ (left) and reheating process at a rate of 10 °C min⁻¹ (right) (a, b) BS/PS = 7/3 - 0, (c, d) BS/PS = 7/3 - 0.01, (e, f) BS/PS = 7/3 - 0.02, (g, h) BS/PS = 7/3 - 0.03



crystallinity. Therefore, a driving force was endowed to the molecular chain in the amorphous state, and thus the chain can be easily folded into an ordered state during the reheating process. Consequently, recrystallization occurs during the reheating process, and the same degree of crystallinity is achieved by obtaining a similar ΔH_m value.

Nonisothermal crystallization kinetics based on the Avrami model

The fraction of relative crystallinity ($X(t)$) as a function of time was calculated, and the results were presented in Fig. S4. The curve of $\log\{-\ln[1-X(t)]\}$ versus $\log(t)$ was performed to obtain the Avrami exponent n and the crystallization rate constant from the slope and the intercept via linear regression and was revealed in Fig. S5 and summarized in Table 4.

Plots of growth rate (G) of PBSPS copolymers in the nonisothermal process at different cooling rates are displayed in Fig. S6. As illustrated in Table 4, the sample with $GC=0.02$ mol% has a higher crystallization rate than $GC=0$ mol% at every cooling rate in $BS/PS=10/0(PBS)$ and $8/2$. However, $BS/PS=7/3$ with different GC concentrations display a different tendency, suggesting the G values are sorted with GC concentration in 0.01 mol% (0.194 min^{-1}) $>$ 0.02 mol% (0.169 min^{-1}) $>$ 0.03 mol% (0.122 min^{-1}) $>$ 0 mol% (0.086 min^{-1}) under a $2.5 \text{ }^\circ\text{C min}^{-1}$ cooling rate. Furthermore, the G values of samples with $GC=0$ mol% (0.487 min^{-1}) and 0.03 mol% (0.505 min^{-1}) under a $10 \text{ }^\circ\text{C min}^{-1}$ cooling rate are higher than for $GC=0.01$ mol% (0.368 min^{-1}) and 0.02 mol% (0.374 min^{-1}). A relatively lower ΔH_{hc} and higher ΔH_{cc} are detected in the $BS/PS=7/3$ when the cooling rate increases, indicating that the crystallization behavior cannot be completed at the given cooling rate. A partial crystallization does not reflect an exact crystallization behavior, which could cause inaccurate results in conventional crystallization kinetics calculation.

Nonisothermal crystallization kinetics based on Mo model

Mo model [46] is also one of the most popular methods to describe the nonisothermal crystallization process as the following equation,

$$\log \emptyset = \log F(T) - a \log t \quad (6)$$

where a is Mo's exponent, $a=(n/m)$.

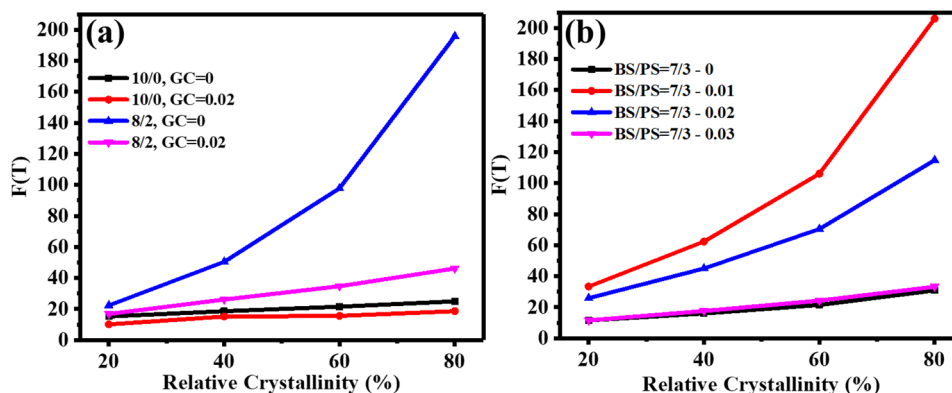
$F(T)$ is a cooling rate parameter when the system reaches a certain degree of crystallinity in a unit of time. Smaller

Table 4 Avrami analysis for nonisothermal crystallization and half-time of crystallization for PBSPS copolymers with GC at different BS/PS concentrations

| Sample | Temp (Φ) | n | K (min^{-n}) | $t_{1/2}$ (min) | G (min^{-1}) |
|------------------------|--------------------|------|------------------------------|--------------------|------------------------------|
| BS/PS = 10/0(PBS)-0 | 2.5 | 5.02 | 0.0002 | 4.93 | 0.202 |
| | 5 | 5.61 | 0.0013 | 3.06 | 0.327 |
| | 7.5 | 5.36 | 0.0105 | 2.19 | 0.457 |
| | 10 | 5.02 | 0.0517 | 1.68 | 0.596 |
| BS/PS = 10/0(PBS)-0.02 | 2.5 | 4.55 | 0.0016 | 3.77 | 0.265 |
| | 5 | 4.31 | 0.0300 | 2.07 | 0.483 |
| | 7.5 | 4.47 | 0.0769 | 1.63 | 0.612 |
| | 10 | 4.48 | 0.1811 | 1.35 | 0.741 |
| BS/PS = 8/2-0 | 2.5 | 3.60 | 0.0008 | 6.56 | 0.152 |
| | 5 | 2.62 | 0.0161 | 4.20 | 0.237 |
| | 7.5 | 2.49 | 0.0284 | 3.60 | 0.277 |
| | 10 | 2.33 | 0.0557 | 2.95 | 0.338 |
| BS/PS = 8/2-0.02 | 2.5 | 3.93 | 0.0026 | 4.12 | 0.243 |
| | 5 | 3.83 | 0.0153 | 2.70 | 0.370 |
| | 7.5 | 3.65 | 0.0461 | 2.10 | 0.476 |
| | 10 | 3.15 | 0.1694 | 1.56 | 0.639 |
| BS/PS = 7/3-0 | 2.5 | 2.32 | 0.0023 | 11.68 | 0.086 |
| | 5 | 2.04 | 0.0168 | 6.19 | 0.162 |
| | 7.5 | 1.85 | 0.0727 | 3.36 | 0.297 |
| | 10 | 1.8 | 0.1895 | 2.05 | 0.487 |
| BS/PS = 7/3-0.01 | 2.5 | 3.88 | 0.0012 | 5.14 | 0.194 |
| | 5 | 3.63 | 0.0065 | 3.62 | 0.277 |
| | 7.5 | 3.28 | 0.0182 | 3.04 | 0.329 |
| | 10 | 3.03 | 0.0337 | 2.71 | 0.368 |
| BS/PS = 7/3-0.02 | 2.5 | 3.55 | 0.0012 | 5.91 | 0.169 |
| | 5 | 3.27 | 0.0040 | 4.84 | 0.207 |
| | 7.5 | 2.89 | 0.0178 | 3.54 | 0.283 |
| | 10 | 2.76 | 0.0454 | 2.68 | 0.374 |
| BS/PS = 7/3-0.03 | 2.5 | 3.32 | 0.0006 | 8.16 | 0.122 |
| | 5 | 2.73 | 0.0084 | 5.03 | 0.198 |
| | 7.5 | 2.28 | 0.0594 | 2.93 | 0.340 |
| | 10 | 2.04 | 0.1718 | 1.97 | 0.505 |

values of $F(T)$ reflect that higher crystallization rates can be obtained. The curve of $\log \emptyset$ versus $\log t$ was collected and presented in Fig. S7. Mo's exponent and $F(T)$ can be calculated from the curve's slope and intercept. The results are displayed in Table S3. Plots of $F(T)$ as a function of relative crystallinity for PBSPS copolymers are displayed in Fig. 9. The values of $F(T)$ for $BS/PS=10/0(PBS)$ and $8/2$ with $GC=0.02$ mol% is lower than those with $GC=0$ mol% at any relative crystallinity, which demonstrates that incorporation with $GC=0.02$ mol% increases the crystallization rate of $BS/PS=10/0(PBS)$ polymers and $8/2$ copolymers. These results corroborate the isothermal crystallization kinetics assessment results. However, for $BS/$

Fig. 9 Plots of $F(T)$ as a function of relative crystallinity for PBSPS copolymers (a) BS/PS = 10/0(PBS) and 8/2 (b) BS/PS = 7/3



PS = 7/3 copolymers, then $F(T)$ for samples with $GC = 0$ and 0.03 mol% is lower than those with $GC = 0.01$ and 0.02 mol%, which is similar to the results of the Avrami model, indicating that partial crystallization behavior could provide nonreasonable, nonreliable results.

Theoretically, the sum of the values of ΔH_{hc} and ΔH_{cc} should be close to ΔH_m . The values recorded in Table S2 reveal that each sample obtained similar values of ΔH_m after cooling and reheating procedures at different rates. The averaged values of ΔH_m are obtained in 39.6 ± 2 , 43.9 ± 2 , 41.5 ± 2 , and $38.7 \pm 2 \text{ J g}^{-1}$ for $GC = 0, 0.01, 0.02$, and 0.03 mol%, respectively. The highest ΔH_m values are observed for $GC = 0.01$ mol% at BS/PS = 7/3, which indicates the highest crystallinity. Furthermore, ΔH_m displayed a comparable value for each sample after different rates of cooling and reheating procedures, suggesting that the crystallization behavior can be accomplished completely in the reheating procedure. The following formula can express the relative crystallinity formed by each sample during different cooling rates,

$$\text{Relative crystallinity at the cooling} = \frac{\Delta H_{hc}}{\Delta H_m} \times 100\% \quad (7)$$

The relative crystallinity at cooling in BS/PS = 7/3 with different GC proportions at varying cooling rates is displayed in Table S2. Plots of relative crystallinity at cooling versus different cooling rates are displayed in Fig. 10a, and a possible mechanism is presented in Fig. 10b. The relative crystallinity at a cooling of $GC = 0.01$ mol% from 92.7% to 83.0% is higher than $GC = 0$ mol% from 78.0% to 13.9% at cooling rates of 2.5 to $10 \text{ }^\circ\text{C min}^{-1}$. The relative crystallinity at cooling in $GC = 0.02$ mol% reduced from 92.4% to 31.6% when the cooling rate was $> 5 \text{ }^\circ\text{C min}^{-1}$. The relative crystallinity is almost the same with $GC = 0$ mol% at cooling rates of 5 and $7.5 \text{ }^\circ\text{C min}^{-1}$, and slightly lower at $10 \text{ }^\circ\text{C min}^{-1}$ in 0.03 mol% GC.

The accumulation of the crosslinking agent can play three roles: (1) the crosslinked points can be considered a nucleation point favoring crystallization; (2) few of the crosslinked points can slightly reduce the kinetic energy of the molecular chain, which is beneficial to chain stacking

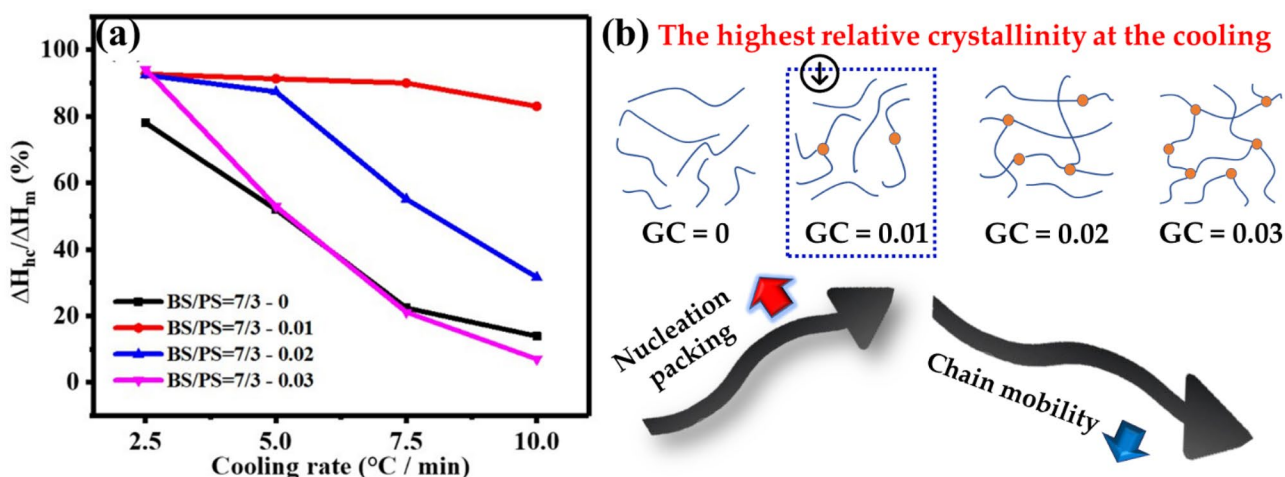


Fig. 10 (a) Plots of relative crystallinity on cooling as a function of different cooling rates for PBSPS = 7/3 copolymers, and (b) a possible mechanism for improving the crystallization rate by a small amount of GC

and crystallization; (3) the segment integrity and mobility of the molecular chain are limited when the number of crosslinked points increases and the molecular chain does not gain enough kinetic energy to stack, which is unfavorable for crystallization [41–43].

When 0.01 mol% GC is employed for BS/PS = 7/3 copolymers, GC is formed as the nucleation point, and the kinetic energy of the molecular chain is slightly reduced. Therefore, crystallization is relatively easy (Relative crystallinity at cooling for GC = 0.01 mol% is 92.7%, 91.3%, 90.0%, and 83.0% at 2.5, 5, 7.5, 10 °C min⁻¹). When 0.02 mol% GC is employed, the nucleating effect increases, and the restriction of chain mobility becomes stronger under a faster cooling rate. Therefore, the relative crystallinity decreases dramatically compared with GC = 0.01 mol%. (Relative crystallinity at cooling for GC = 0.02 mol% is 92.4%, 87.4%, 55.1%, and 31.6% at 2.5, 5, 7.5, 10 °C min⁻¹) When GC is enriched to 0.03 mol%, the hindrance of chain mobility is enhanced. Similar relative crystallinity at cooling with GC = 0 mol% is obtained at a cooling rate of 5 and 7.5 °C min⁻¹ (Relative crystallinity at cooling for GC = 0 mol% is 78.0%, 52.0%, 22.4%, and 13.9%; for GC = 0.03 mol% is 94.1%, 52.9%, 21.1%, and 7.0% at 2.5, 5, 7.5, 10 °C min⁻¹). Furthermore, a higher value of relative crystallinity is observed for GC = 0.01, 0.02, and 0.03 mol% compared with GC = 0 mol% at a cooling rate of 2.5 °C min⁻¹, which demonstrates that the nucleation point increases. Even if the crystal growth is reduced by increasing the GC concentration, the complete crystals can reach relatively high crystallinity when the material has enough time to crystallize.

Conclusions

The crystallization behavior of PBSPS copolymers was systematically explored by isothermal crystallization and nonisothermal crystallization. The higher PS ratio within PBSPS copolymers can directly affect the crystallization rate, which decreases with the increase of the PS ratio. This finding demonstrates that the PS unit on the copolymer chain obstructs the crystallizability of the BS unit. The Avrami exponent is observed in a range of 2.01–3.50, indicating that three-dimensional growth is initiated by a heterogeneous nucleation mechanism. A higher crystallization rate is observed in 0.02 mol% GC than in 0 mol% GC in all PBSPS copolymers. Because molecular chains are challenging to stack into the crystal area at a faster cooling rate, a reduced ΔH_{hc} and a lower crystallinity are observed. A 0.01 mol% GC in BS/PS = 7/3 copolymer acts as a nucleation point, causing the kinetic energy of the molecular chain to be reduced and crystallization to occur rapidly. The use of 0.02 mol% GC in BS/PS = 7/3

copolymer can reduce the mobility of the molecular chain to obtain a lower relative crystallinity at cooling. When GC is improved to 0.03 mol%, the barrier of chain migration is further strengthened, and the relative crystallinity at cooling is similar to 0 mol% at cooling rates of 5 and 7.5 °C min⁻¹. This study demonstrates that the type of crystallization behavior can be controlled by changing the concentration of BS/PS, and adding a small amount of GC concentration. Therefore, the performance of PBSPS copolymers can be improved through the adjustments of the crystallization rate during the preparation process.

Supplementary information The online version contains supplementary material available at <https://doi.org/10.1007/s10965-021-02460-x>.

Acknowledgments The authors gratefully acknowledge the financial support from the Ministry of Science and Technology of Taiwan (MOST 109-2634-F-027-001), (MOST 109-2622-E-027-004 -CC3), and (MOST 109-2221-E-027 -114 -MY3).

References

- Väisänen T, Das O, Tomppo L (2017) A review on new bio-based constituents for natural fiber-polymer composites. *J Clean Prod* 149:582–596. <https://doi.org/10.1016/j.jclepro.2017.02.132>
- Spierling S, Knüpfer E, Behnsen H et al (2018) Bio-based plastics - A review of environmental, social and economic impact assessments. *J Clean Prod* 185:476–491. <https://doi.org/10.1016/j.jclepro.2018.03.014>
- Kawaguchi H, Hasunuma T, Ogino C, Kondo A (2016) Bioprocessing of bio-based chemicals produced from lignocellulosic feedstocks. *Curr Opin Biotechnol* 42:30–39. <https://doi.org/10.1016/j.copbio.2016.02.031>
- Babu RP, O'Connor K, Seeram R (2013) Current progress on bio-based polymers and their future trends. *Prog Biomater* 2:8. <https://doi.org/10.1186/2194-0517-2-8>
- Avella M, Buzarovska A, Errico M et al (2009) Eco-Challenges of Bio-Based Polymer Composites *Materials* 2:911–925. <https://doi.org/10.3390/ma2030911>
- Isikgor FH, Becer CR (2015) Lignocellulosic biomass: a sustainable platform for the production of bio-based chemicals and polymers. *Polym Chem* 6:4497–4559. <https://doi.org/10.1039/C5PY00263J>
- Mekonnen T, Mussone P, Khalil H, Bressler D (2013) Progress in bio-based plastics and plasticizing modifications. *J Mater Chem A* 1:13379. <https://doi.org/10.1039/c3ta12555f>
- McKinlay JB, Vieille C, Zeikus JG (2007) Prospects for a bio-based succinate industry. *Appl Microbiol Biotechnol* 76:727–740. <https://doi.org/10.1007/s00253-007-1057-y>
- Zia KM, Noreen A, Zuber M et al (2016) Recent developments and future prospects on bio-based polyesters derived from renewable resources: A review. *Int J Biol Macromol* 82:1028–1040. <https://doi.org/10.1016/j.ijbiomac.2015.10.040>
- Johansson C, Bras J, Mondragon I et al (2012) Renewable Fibers and Bio-based Materials for Packaging Applications – A Review of Recent Developments. *BioResources* 7:2506–2552. <https://doi.org/10.15376/biores.7.2.2506-2552>
- Hottle TA, Bilec MM, Landis AE (2013) Sustainability assessments of bio-based polymers. *Polym Degrad Stab* 98:1898–1907. <https://doi.org/10.1016/j.polymdegradstab.2013.06.016>

12. Álvarez-Chávez CR, Edwards S, Moure-Eraso R, Geiser K (2012) Sustainability of bio-based plastics: general comparative analysis and recommendations for improvement. *J Clean Prod* 23:47–56. <https://doi.org/10.1016/j.jclepro.2011.10.003>
13. Yin G-Z, Yang X-M (2020) Biodegradable polymers: a cure for the planet, but a long way to go. *J Polym Res* 27:38. <https://doi.org/10.1007/s10965-020-2004-1>
14. Papageorgiou GZ, Bikiaris DN (2005) Crystallization and melting behavior of three biodegradable poly(alkylene succinates). A comparative study *Polymer* 46:12081–12092. <https://doi.org/10.1016/j.polymer.2005.10.073>
15. Papageorgiou GZ, Achilias DS, Bikiaris DN (2007) Crystallization Kinetics of Biodegradable Poly(butylene succinate) under Isothermal and Non-Isothermal Conditions. *Macromol Chem Phys* 208:1250–1264. <https://doi.org/10.1002/macp.200700084>
16. Jin T, Zhou M, Hu S et al (2014) Effect of molecular weight on the properties of poly(butylene succinate). *Chin J Polym Sci* 32:953–960. <https://doi.org/10.1007/s10118-014-1463-4>
17. Yoo ES, Im SS (1999) Melting behavior of poly(butylene succinate) during heating scan by DSC. *J Polym Sci Part B Polym Phys* 37:1357–1366
18. Xu J, Guo B-H (2010) Microbial Succinic Acid, Its Polymer Poly(butylene succinate), and Applications. In: Chen GG-Q (ed) *Plastics from Bacteria*. Springer Berlin Heidelberg, Berlin, Heidelberg, pp 347–388
19. Xu J, Guo B-H (2010) Poly(butylene succinate) and its copolymers: Research, development and industrialization. *Biotechnol J* 5:1149–1163. <https://doi.org/10.1002/biot.201000136>
20. Gigli M, Fabbri M, Lotti N et al (2016) Poly(butylene succinate)-based polyesters for biomedical applications: A review. *Eur Polym J* 75:431–460. <https://doi.org/10.1016/j.eurpolymj.2016.01.016>
21. Gan Z, Abe H, Kurokawa H, Doi Y (2001) Solid-State Microstructures, Thermal Properties, and Crystallization of Biodegradable Poly(butylene succinate) (PBS) and Its Copolyesters. *Biomacromol* 2:605–613. <https://doi.org/10.1021/bm015535e>
22. Yang Y, Qiu Z (2011) Crystallization kinetics and morphology of biodegradable poly(butylene succinate-*co*-ethylene succinate) copolyesters: effects of comonomer composition and crystallization temperature. *CrystEngComm* 13:2408. <https://doi.org/10.1039/c0ce00598c>
23. Liu F-Y, Xu C-L, Zeng J-B et al (2013) Non-isothermal crystallization kinetics of biodegradable poly(butylene succinate-*co*-diethylene glycol succinate) copolymers. *Thermochim Acta* 568:38–45. <https://doi.org/10.1016/j.tca.2013.06.025>
24. Wang G, Qiu Z (2012) Synthesis, Crystallization Kinetics, and Morphology of Novel Biodegradable Poly(butylene succinate-*co*-hexamethylene succinate) Copolyesters. *Ind Eng Chem Res* 51:16369–16376. <https://doi.org/10.1021/ie302817k>
25. Dai X, Qiu Z (2017) Crystallization kinetics, morphology, and hydrolytic degradation of novel biobased poly(butylene succinate-*co*-decamethylene succinate) copolyesters. *Polym Degrad Stab* 137:197–204. <https://doi.org/10.1016/j.polymdegradstab.2017.01.020>
26. Chen C-H, Yang C-S, Chen M et al (2011) Synthesis and characterization of novel poly(butylene succinate-*co*-2-methyl-1,3-propylene succinate)s. *Express Polym Lett* 5:284–294. <https://doi.org/10.3144/expresspolymlett.2011.29>
27. Lu J-S, Chen M, Lu S-F, Chen C-H (2011) Nonisothermal crystallization kinetics of novel biodegradable poly(butylene succinate-*co*-2-methyl-1,3-propylene succinate)s. *J Polym Res* 18:1527–1537. <https://doi.org/10.1007/s10965-010-9558-2>
28. Xie W-J, Zhou X-M (2015) Non-isothermal crystallization kinetics and characterization of biodegradable poly(butylene succinate-*co*-neopentyl glycol succinate) copolyesters. *Mater Sci Eng C* 46:366–373. <https://doi.org/10.1016/j.msec.2014.10.063>
29. Bikiaris DN, Papageorgiou GZ, Papadimitriou SA et al (2009) Novel Biodegradable Polyester Poly(Propylene Succinate): Synthesis and Application in the Preparation of Solid Dispersions and Nanoparticles of a Water-Soluble Drug. *AAPS PharmSciTech* 10:138–146. <https://doi.org/10.1208/s12249-008-9184-z>
30. Bikiaris DN, Achilias DS (2006) Synthesis of poly(alkylene succinate) biodegradable polyesters I. Mathematical modelling of the esterification reaction. *Polymer* 47:4851–4860. <https://doi.org/10.1016/j.polymer.2006.04.044>
31. Chrissafis K, Paraskevopoulos KM, Bikiaris DN (2006) Thermal degradation kinetics of the biodegradable aliphatic polyester, poly(propylene succinate). *Polym Degrad Stab* 91:60–68. <https://doi.org/10.1016/j.polymdegradstab.2005.04.028>
32. Papageorgiou GZ, Bikiaris DN (2007) Synthesis, Cocrystallization, and Enzymatic Degradation of Novel Poly(butylene-*co*-propylene succinate) Copolymers. *Biomacromol* 8:2437–2449. <https://doi.org/10.1021/bm0703113>
33. Xu Y, Xu J, Liu D et al (2008) Synthesis and characterization of biodegradable poly(butylene succinate-*co*-propylene succinate)s. *J Appl Polym Sci* 109:1881–1889. <https://doi.org/10.1002/app.24544>
34. Xu Y, Xu J, Guo B, Xie X (2007) Crystallization kinetics and morphology of biodegradable poly(butylene succinate-*co*-propylene succinate)s. *J Polym Sci Part B Polym Phys* 45:420–428. <https://doi.org/10.1002/polb.20877>
35. Lu S-F, Chen M, Shih Y-C, Chen CH (2010) Nonisothermal crystallization kinetics of biodegradable poly(butylene succinate-*co*-propylene succinate)s. *J Polym Sci Part B Polym Phys* 48:1299–1308. <https://doi.org/10.1002/polb.22027>
36. Chan H, Cho C, Hsu K et al (2019) Smart Wearable Textiles with Breathable Properties and Repeatable Shaping in In Vitro Orthopedic Support from a Novel Biomass Thermoplastic Copolyester. *Macromol Mater Eng* 304:1900103. <https://doi.org/10.1002/mame.201900103>
37. Chen C-W, Hsu T-S, Rwei S-P (2019) Effect of Ethylenediaminetetraacetic Acid on Unsaturated Poly(Butylene Adipate-*Co*-Butylene Itaconate) Copolyester with Low-Melting Point and Controllable Hardness. *Polymers* 11:611. <https://doi.org/10.3390/polym11040611>
38. Cho C-J, Chang Y-S, Lin Y-Z et al (2020) Green electrospun nanofiber membranes filter prepared from novel biomass thermoplastic copolyester: Morphologies and filtration properties. *J Taiwan Inst Chem Eng* 106:206–214. <https://doi.org/10.1016/j.jtice.2019.11.002>
39. Chen C-W, Hsu T-S, Huang K-W, Rwei S-P (2020) Effect of 1,2,4,5-Benzenetetracarboxylic Acid on Unsaturated Poly(butylene adipate-*co*-butylene itaconate) Copolyesters: Synthesis, Non-Isothermal Crystallization Kinetics, Thermal and Mechanical Properties *Polymers* 12:1160. <https://doi.org/10.3390/polym12051160>
40. Hsu K-H, Chen C-W, Wang L-Y et al (2019) Bio-based thermoplastic poly(butylene succinate-*co*-propylene succinate) copolyesters: effect of glycerol on thermal and mechanical properties. *Soft Matter* 15:9710–9720. <https://doi.org/10.1039/C9SM01958H>
41. Liu G-C, Zhang W-Q, Zhou S-L et al (2016) Improving crystallization and processability of PBS via slight cross-linking. *RSC Adv* 6:68942–68951. <https://doi.org/10.1039/C6RA13488B>
42. Liu G-C, Zhang W-Q, Wang X-L, Wang Y-Z (2017) Synthesis and performances of poly(butylene-succinate) with enhanced viscosity and crystallization rate via introducing a small amount of diacetylene groups. *Chin Chem Lett* 28:354–357. <https://doi.org/10.1016/j.ccl.2016.10.014>
43. Ma P, Ma Z, Dong W et al (2013) Structure/Property Relationships of Partially Crosslinked Poly(butylene succinate). *Macromol Mater Eng* 298:910–918. <https://doi.org/10.1002/mame.201200209>
44. Avrami M (1940) Kinetics of Phase Change. II Transformation-Time Relations for Random Distribution of Nuclei. *J Chem Phys* 8:212–224. <https://doi.org/10.1063/1.1750631>

45. Pivsa-Art W, Fujii K, Nomura K, Aso Y, Ohara H, Yamane H (2016) Isothermal crystallization kinetics of talc-filled poly(lactic acid) and poly(butylene succinate) blends. *J Polym Res* 23:144. <https://doi.org/10.1007/s10965-016-1045-y>
46. Liu T, Mo Z, Wang S, Zhang H (1997) Nonisothermal melt and cold crystallization kinetics of poly(aryl ether ether ketone). *Polym Eng Sci* 37:568–575. <https://doi.org/10.1002/pen.11700>
47. Durmus A, Yalçinyuva T (2009) Effects of additives on non-isothermal crystallization kinetics and morphology of isotactic polypropylene. *J Polym Res* 16:489–498. <https://doi.org/10.1007/s10965-008-9252-9>
48. Chen C-W, Hsu T-S, Rwei S-P (2020) Isothermal Kinetics of Poly(butylene adipate-*co*-butylene itaconate) Copolyesters with Ethylenediaminetetraacetic Acid. *ACS Omega* 5:3080–3089. <https://doi.org/10.1021/acsomega.9b04315>

Publisher's Note Springer Nature remains neutral with regard to jurisdictional claims in published maps and institutional affiliations.